ELSEVIER

The Chemical Engineering Journal 64 (1996) 99–106

THE CHEMICAL ENGINEERING JOURNAL

Rheological modeling of fractal and dense suspensions

Romano Lapasin *, Mario Grassi, Sabrina Pricl

Department of Chemical, Environmental and Raw Materials Engineering, University of Trieste, Piazzale Europa 1, Trieste I-34127, Italy

Abstract

The development of a rheological model for aggregated suspensions is necessarily based upon a suitable characterization of the structure of the disperse phase and of the structural modifications produced by a deformation or a velocity field. The disperse phases of real aggregate particle suspensions, both dilute and concentrated, may present a wide variety of structures, which can be conveniently characterized by using the concepts of fractal geometry. In the present paper we formulate a rheological model able to correlate the structural processes induced by shear flow conditions and the consequent shear dependence of viscosity with the shear stress changes experienced by the suspension. The flow curves calculated from the model, both for dense and fractal aggregates, closely resemble those observed for real colloidal and non-colloidal suspensions. The model appears particularly advantageous in describing the transition from shear thinning to plastic behavior, which usually occurs with increasing volume fraction or aggregation of the disperse phase. The role played by the aggregation state of the disperse phase becomes predominant in the low shear stress range, where aggregates may be composed of many particles, and, consequently, where the fractal dimensionality D becomes an important parameter in determining the compactness of the aggregate structure and the rheological behavior of concentrated suspensions. The validity of the proposed model is checked further through an analysis of experimental viscosity data relative to two series of epoxy–acrylic systems, containing titanium dioxide and aluminum silicate at different disperse phase concentrations.

Keywords: Rheological modeling; Fractal suspensions; Dense suspensions; Aggregated suspensions

1. Introduction

Suspension rheology is an attractive argument for both scientists and technologists. Several stimulating aspects for scientists arise from the non-linear properties exhibited by concentrated suspensions, such as shear thinning, and shear thickening, yield stress and thixotropy, and from the structural features of the disperse phase and its modifications under flow conditions which are essentially produced by ordering and aggregation processes. On the other hand, suspension rheology represents a useful tool for control and optimization in the formulation of industrial products and plays a crucial role in the analysis and control of processing and transportation as well.

At present, industrial problems are usually tackled and solved by resorting to experimental tests and simple empirical correlations which are suitable to describe the main phenomenological aspects with an acceptable approximation. Indeed, an optimum condition should be achieved if the rheological properties of suspensions would be derived directly from the structural features of the disperse phase on the microscale and mesoscale. In this manner, the solutions of industrial problems could be intrinsically combined with a physical interpretation of the rheological effects connected with the formulation and processing of the suspensions. Such a task appears to be laborious and intricate especially when the disperse phase is composed of particle aggregates or flocs and this structural condition is frequently observed in many industrial suspensions.

Particle interactions and hydrodynamic coupling together with the Brownian motion and an imposed flow field lead to the spatial correlation between particles, which in turn determines the non-linear rheological behavior of a suspension. While a repulsive interaction leads to an ordered liquid-like structure for sufficiently high particle concentrations, an attractive interaction may lead to the formation of particle clusters and even to continuous networks. The aggregation state of the disperse phase is determined by a number of factors, essentially bound to the geometric and surface features of the particles (dimensions, shape, presence of charges or adsorbed components), to their numerical density and to the specific field condition (temperature, hydrodynamic conditions, presence of other components in the fluid phase). In the absence of an effective stabilizing action (of electrostatic and/or steric nature), particles do aggregate among them-

* Corresponding author.

PII S0923-0467(96)03107-7

selves to an extent which is mainly a function of the particle dimensions. Thus, particle aggregation may lead to the formation of very large particle clusters in colloidal systems. These random tenuous structures can be properly treated as fractal objects because they are self-similar and remain invariant under a change of length scale. Even in coarse particle suspensions, however, a temporary aggregation state can eventually be observed, depending on particle concentration and intensity of the applied velocity field [1].

The structural alterations of particle aggregates accompanying the application of a stress field are the main factors responsible for the non-linear properties of aggregated dilute and concentrated suspensions. At rest, when particle concentration is sufficiently high, the aggregated disperse phase may span the entire space from wall to wall, thus conferring to the system those mechanical characteristics typical of a gel state, whereas, under flow conditions, it breaks down into smaller clusters, having shapes and dimensions which change from system to system and with the intensity of flow. Correspondingly, the viscosity decreases with increasing shear rate or shear stress, and this shear dependence is also a function of the disperse phase concentration. Thus, the development of a model correlating the macroscopic properties and the microscopic features of aggregated suspensions is necessarily based upon a suitable characterization of the structure of the disperse phase and of the structural modifications produced by a deformation or a velocity field.

The disperse phase of real aggregated suspensions, both dilute and concentrated, may present a wide variety of structures, depending on the specific characteristics of the particles and the different factors which affect the particle–particle interaction potential and, hence, govern the aggregation state. Particle aggregations have been the subject of many experimental and theoretical studies, since they are of utmost importance in many branches of science and technology, especially in the colloid science area [2–20]. Aggregates having different size and density can be simulated through computer calculations by assuming different aggregation mechanisms. One of the earliest models for the computer simulation of aggregate formation in three dimensions was introduced by Vold [2]. According to this model, particles following random linear trajectories are added to a growing cluster of particles at the position where they first contact the cluster. Vold's work opens a long series of simulation studies in two- and three-dimensional space, based upon different aggregation mechanisms.

All these analyses have been extended to very large clusters, having colloidal aggregates as reference systems; consequently, the concept of fractal dimensionality has been conveniently used to interpret the results of the computer simulations and to characterize the aggregate structure. This idea is a particularly valuable way of describing many of the geometrical properties of structures which are self-similar or statistically self-similar. For sufficiently large cluster sizes, the dependence of the radius of gyration R_g on the number of particles in the cluster n can be expressed as $R_g \sim n^{1/D}$, where D is the fractal dimension. Similar scaling laws can be written for other geometric quantities: among them, an important quantity which characterizes self-similar objects is the density correlation function $C(r)$, where r is the distance from the center of mass of the cluster. If the object has fractal dimension D and is embedded in a d-dimensional Euclidean space, then $C(r) \sim r^{(D-d)}$.

The fractal dimension has important implications for colloidal systems: if $D < d$, the density of the cluster will become smaller and smaller as the cluster grows larger and larger. The D value obtained for fractal aggregates generated with different mechanisms in a three-dimensional Euclidean space ranges between 1.78 and 2.1, passing from diffusion-limited cluster–cluster aggregation to reaction-limited cluster–cluster aggregation [16,17]. When reordering processes (bending, folding and twisting) are combined with the different aggregation mechanisms, more compact aggregates are obtained from computer simulation, and, hence, the relevant D values are higher and confined in a narrow range, between 2.18 and 2.25 [17]. When the particle size distribution is wide and particles are closely arranged within the cluster, the void fraction of each aggregate is negligible. For these dense aggregates the fractal and Euclidean dimensions coincide ($D = d = 3$).

The fractal dimension D can be properly used as a measure of the density of the aggregated disperse phase only if particle aggregates are very extended and self-similar within a length interval comprised between two cut-off limits and, hence, treated as fractal objects. All the above scaling laws cannot be extended to smaller degrees of aggregation, which are typical of several coarse suspensions in any flow conditions or may be encountered even in colloidal systems at high shear rates. For smaller aggregates, generated with a given mechanism of aggregation, the radius of gyration R_g increases with the particle number n but its derivative $\mathrm{d} \log D / \mathrm{d} \log n$ decreases with increasing n, tending to $1/D$ only for sufficiently high n.

In real systems the size distribution of particle aggregates is frequently wide so that the disperse phase may be composed of fractal and smaller aggregates, which are produced by the same aggregation mechanism. Even if the density of the individual aggregates may be significantly different, the whole aggregate ensemble can be suitably characterized with the D value, associated with the relevant aggregation mechanism. Nevertheless, we must notice that different scaling laws (D values) can be derived from the same mechanism of aggregation, only by adjusting some parameters of the model, as for clustering of clusters, which is a basic aggregation model applicable to several colloidal systems. Moreover, the aggregation mechanism may change with increasing concentration of the disperse phase, with a corresponding change of the fractal dimensionality. Accordingly, the only objective we can wisely pursue in order to achieve a suitable characterization of the structure of the disperse phase is the definition of a general functional dependence for $R_g(n)$ or other related quantities, valid for all n values and for different aggregation

mechanisms. This functional dependence should contain few adjustable parameters, connected with the aggregation mechanism and, hence, with the fractal dimension D. Such a goal can be reached through the analysis of the experimental data relative to real dense aggregates and of the numerical results obtained from computer simulations based upon different mechanism of aggregation, as it will be shown hereafter.

In the present paper we illustrate the development of a rheological model suitable to describe the dependence of the viscosity on the shear stress and on the disperse phase concentration for suspensions of particle aggregates, having different features and densities, ranging from those peculiar to fractal clusters to those typical of dense aggregates. The model contains four adjustable parameters which are strictly connected with the compactness and the shear resistance of particle aggregates. Moreover, we present the results obtained from the application of the model to experimental data relative to industrial pigment suspensions, having different disperse phase concentrations and composed of different pigment particles.

2. Rheological modeling of aggregated suspensions

The fundamental objective of the rheological modeling is the definition of an equation able to describe the dependence of the viscosity η on the shear stress τ and on the disperse phase concentration Φ. The modeling procedure can be divided into several steps, the first concerning the choice of an adequate functional dependence of viscosity on disperse phase concentration.

2.1. Dependence of the viscosity on the effective volume fraction of the disperse phase

The relationship between the viscosity of suspensions of non-interacting particles and the volume fraction of the disperse phase is generally expressed as:

$$\eta = \eta_s \eta_r(\Phi) \tag{1}$$

where η_s is the viscosity of the continuous phase, and η_r is the relative viscosity, which characterizes the contribution of the disperse phase and is an increasing function of Φ.

Among the several models proposed for $\eta_r(\Phi)$, particular mention is made of the Quemada model [21], which can be written in the two equivalent forms:

$$\eta_r = (1 - \Phi/\Phi_m)^{-2} = \left(1 - \frac{[\eta]}{2}\Phi\right)^{-2} \tag{2}$$

where Φ_m is the maximum packing volume fraction and $[\eta]$ is the intrinsic viscosity. The Quemada equation was derived starting from the optimization of the viscous energy dissipation and can be considered a particular case of the more general relationship suggested by Krieger and Dougherty [22]:

$$n_r = (1 - \Phi/\Phi_m)^{-[\eta]\Phi_m} \tag{3}$$

for $[\eta]\Phi_m = 2$. This condition is often verified in the application of Eq. (3) to many real suspensions. Both $[\eta]$ and Φ_m, which are strictly correlated in the Quemada equation, depend on the particle shape and size distribution and are function of the applied shear stress or shear rate. For increasing shear stresses, the space distribution of the particles becomes more ordered, forming layers and strings in the flow direction, so leading to increasing values of Φ_m. Accordingly, a model can be formulated for the description of the shear dependence of viscosity of stabilized particles, which is based upon the shear dependence of Φ_m [23].

At any flow condition, the viscosity of an aggregated suspension is assumed to depend primarily on the effective volume of the disperse phase Φ_{eff}, which in its turn depends on the degree of aggregation of the solid particles. The main effect resulting from the aggregation processes is an increase in volume of the disperse phase with respect to its nominal value, i.e. the sum of the volumes of the constituent particles. A global measure of the volume increase of the disperse phase is given by the parameter C_{fp}, defined as:

$$C_{fp} = \frac{\Phi_{eff}}{\Phi} \tag{4}$$

The parameter C_{fp} depends on the mechanism of aggregation and on the number of particles per aggregate. Its value is closer to 1 for more dense aggregates and decreases with decreasing particle number.

If we neglect the effects bound to aggregate anisometry and their subsequent orientation in the flow field, changes of the stress field result only in disperse phase aggregation and breakdown processes and, hence, into changes of Φ_{eff} and C_{fp}. Another assumption useful to model development is concerned with the shape and nature of the aggregates, which may be regarded as impenetrable spheres. Even if the permeability of aggregates can be taken into account, however, the depth of liquid penetration into the aggregate is relatively small, so that the assumption of permeable aggregates exceeds the precision of the assumption regarding their form [24]. As a consequence, we can reasonably extend the validity of the Quemada model to the case of aggregated suspensions, provided we substitute Φ with Φ_{eff} (or C_{fp}):

$$\eta_r = (1 - C_{fp}\Phi/\Phi_m)^{-2} = \left(1 - \frac{C_{fp}[\eta]}{2}\Phi\right)^{-2} \tag{5}$$

Moreover, we suppose that $[\eta]$ and Φ_m are independent of flow conditions, and that is equivalent to assume that the shape and size distribution of the aggregates do not depend appreciably from the applied shear stress or shear rate, if compared with Φ_{eff} and C_{fp}. Accordingly, the shear dependence of viscosity can be derived from the Quemada equation on condition that the shear dependence of C_{fp} is defined.

2.2. Dependence of the effective volume fraction on the degree of aggregation

A further step in the derivation of the rheological model consists of defining the functional dependence of the effective volume of the disperse phase Φ_{eff} (and C_{fp}) on the degree of aggregation (i.e. on the average or maximum number of particles per aggregate).

For a cluster made up by n_i monosized spherical particles of radius a, the dependence of C_{fp} on n_i can be written as follows:

$$C_{fp_i}=\frac{V_i}{n_i V_p}=\frac{R_i^3}{n_i a^3} \tag{6}$$

where V_i and V_p are the volume of the cluster and the volume of the particle, respectively, and R_i is the equivalent hydrodynamic radius of the cluster.

In the case of fractal aggregates, if we assume the hydrodynamic radius R_i to be proportional to the cluster radius of gyration R_g, we obtain:

$$R_i \sim n_i^{1/D} \quad C_{fp_i} \sim n_i^{\beta} \tag{7}$$

with $\beta=3/D-1$. When $D<3$, the density of the floc decreases with increasing n_i.

Eq. 7 holds only for fractal aggregates, but, in flow conditions, the disperse phase of real systems may be composed of aggregates having quite different sizes, ranging from primary particles to very extended clusters. Thus, we must define a relationship suitable to describe the dependence of C_{fp} on n_i with acceptable approximation in the whole n_i range ($n_i \geq 1$) and convergent to Eq. (7) for sufficiently high n_i. To this purpose, we analyzed data obtained from computer simulations for the radius of gyration of aggregates generated according to the ballistic cluster–cluster aggregation mechanism (BCCA) [17], assumed as a representative aggregation process for several real fractal systems, and experimental data relative to suspensions of sintered glass particles [25], corresponding to the other extreme case of dense aggregates (DA). In both cases a satisfactory data correlation was achieved with the following expression:

$$C_{fp_i}=\frac{B+A(a_i^{\beta+1}-1)}{B+n_i-1} \tag{8}$$

Fig. 1 shows the good quality of the fitting achieved with Eq. (8) in these two extreme cases. The values of the parameters B, A and β are 4.965, 2.035 and 0 (for DA) and 1.72, 1.172 and 0.538 (for BCCA), respectively. In the first case, A represents the limiting value of C_{fp} for $n_i \to \infty$; in the second case, for n_i large enough ($n_i > 50$), C_{fp} tends to the same scaling law indicated by Eq. (7), being $D=1.95$. The functional dependence expressed by Eq. (8) provides satisfactory results also in the analysis of other aggregation mechanisms. As an example, a good correlation of numerical data obtained for reaction limited cluster–cluster aggregation mechanism (RLCCA) is obtained for $B=2.705$, $A=2.189$ and $\beta=0.435$. The β value is consistent with the dimension D of the corresponding fractal aggregates ($D=2.09$). Thus, we can sensibly conclude that the functional dependence expressed by Eq. (8) is valid independently of the particular aggregation mechanism involved.

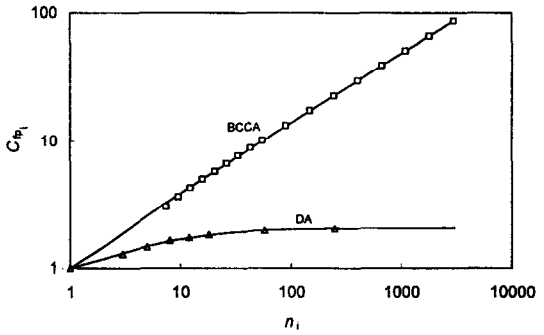

Fig. 1. Comparison (DA) between experimental data for dense aggregates (□) and model prediction (solid line) according to Eq. (8) ($\beta=0$, $A=2.035$, $B=4.965$) and (BCCA) between computer simulated data for ballistic clustering aggregation (△) and model prediction (solid line) according to Eq. (8) ($\beta=0.538$, $A=1.172$, $B=1.72$).

In the case of monosized spherical aggregates, the value of C_{fp} for the global suspension coincides with that of each single cluster. Nevertheless, the real situation is characterized by an aggregate size distribution, variable with imposed flow conditions, which must satisfy the mass balance:

$$N=\sum_{n_i=N_{min}}^{N_{max}} \upsilon_i n_i \tag{9}$$

where N is the total number of the particles in the system and ν_i is the number of aggregates composed of n_i particles.

Accordingly, we obtain:

$$C_{fp}=\frac{\sum_{n_i=N_{min}}^{N_{max}} \upsilon_i V_i}{NV_p}=\frac{1}{N}\sum_{n_i-N_{min}}^{N_{max}} \upsilon_i \left(\frac{R_i}{a}\right)^3=\frac{1}{N}\sum_{n_i=N_{min}}^{N_{max}} \upsilon_i n_i C_{fp_i} \tag{10}$$

In the present work we assume the following hyperbolic size distribution $\nu_i(n_i)$:

$$\nu_i=\frac{N}{N_{max}-N_{min}+1}\frac{1}{n_i} \tag{11}$$

which satisfies the condition set by Eq. (9) and provides a satisfactory approximation to several real size distributions.

From Eqs. (9) and (11) we obtain, in the case of maximum generality ($N_{min}=1$):

$$C_{fp}=\frac{1}{N_{max}}\sum_{n_i=1}^{N_{max}} C_{fp_i} \tag{12}$$

Combining Eqs. (7) and (12) yields:

$$C_{fp}=\frac{1}{N_{max}}\sum_{n_i=1}^{N_{max}}\frac{B+A(n_i^{\beta+1}-1)}{B+n_i-1} \tag{13}$$

To simplify the successive steps involved in model development, we can resort to an approximated expression of Eq.

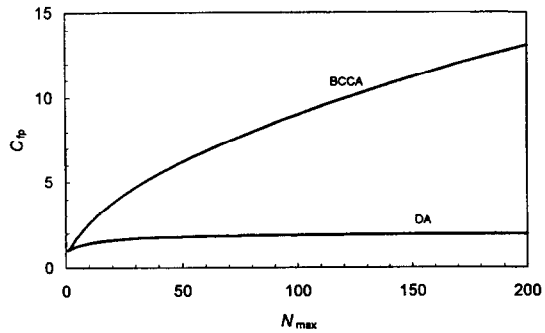

Fig. 2. Profiles of c_{fp} vs. N_{max} calculated from Eq. (14) for DA suspensions ($\bar{A}=1.986$, $\bar{B}=12.40$ and $\bar{\beta}=0$) and BCCA suspensions ($\bar{A}=0.760$, $\bar{B}=1.574$ and $\bar{\beta}=0.538$).

(13), containing N_{max} as the independent variable and having the same functional dependence of Eq. (8):

$$C_{fp}=\frac{\bar{B}+\bar{A}(N_{max}^{\bar{\beta}+1}-1)}{\bar{B}+N_{max}-1} \tag{14}$$

where the values of $\bar{B}, \bar{A}$ and $\bar{\beta}$ are 12.40, 1.986 and 0 for DA and 1.574, 0.760 and 0.538 for BCCA, respectively. Fig. 2 reports the profiles of C_{fp} vs. N_{max} for DA and BCCA systems. Equivalent results are obtained if the reference variable is the average number of particle per aggregate $\bar{n}$.

2.3. Dependence of the degree of aggregation on the shear stress

In order to complete the rheological modeling is now sufficient to define the dependence of N_{max} on the shear stress or the shear rate, provided that changes in the flow conditions do not affect the hyperbolic size distribution law except for its amplitude (i.e. N_{max}). Otherwise, also the variation of Φ_m (or $[\eta]$) with shear flow conditions should be taken into account. In the present work we adopted the shear stress as independent variable, since this choice enables us to predict the appearance of an yield stress at sufficiently high concentration and/or aggregation of the disperse phase. In this sense, the present version represents an improvement of the previous formulation [26].

Several theoretical analyses and experimental observations have been performed on the stress state within particle aggregates, their structure and breakdown under shearing flow conditions [27–36]. Here, the functional dependence of N_{max} on τ is simply derived from the following rate equation which expresses the balance between the particle aggregation and aggregate breakdown processes:

$$\frac{dN_{max}}{dt}=a(N-N_{max})-b\tau^{p}(N_{max}-N_{max,\infty}) \tag{15}$$

where $N_{max,\infty}$ represents the lower limit to which N_{max} tends for $\tau\rightarrow\infty$. The aggregation process is assumed to be independent of the applied shear stress, so that the rate constant a depends only on temperature. The aggregate breakdown process is favored by high shear conditions and, hence, its rate constant increases with increasing shear stress, being $p>0$. Under steady state conditions, we obtain, for $N>>N_{max}$:

$$N_{max}=N_{max,\infty}+\frac{aN}{b}\tau^{-p}=N_{max,\infty}+\left(\frac{\tau}{\tau_c}\right)^{-p} \tag{16}$$

Such a functional dependence of $N_{max}(\tau)$ is in accordance with experimental observations on the variations of aggregate size under shear flow conditions [31–34].

Combining Eqs. (5), (14) and (16) leads to the final expressions for the viscosity as a function of the disperse phase volume fraction and the shear stress, respectively:

$$\eta=\eta_s\left\{1-\frac{\Phi}{\Phi_m}\frac{\bar{B}+\bar{A}[(n_{max,\infty}+(\tau/\tau_c)^{-p})^{\bar{\beta}+1}-1]}{\bar{B}+N_{max,\infty}+(\tau/\tau_c)^{-p}-1}\right\}^{-2} \tag{17}$$

$\bar{B}, \bar{A}$ and $\bar{\beta}$ are connected with the density of particle aggregates which is governed by the mechanism of aggregation. Lower values of all these parameters correspond to lower density of particle aggregates (lower fractal dimension D). $N_{max,\infty}$ gives a measure of structural state of the suspension in high shear conditions. When all the aggregates are broken down to primary particles at very high shear stresses, $N_{max,\infty}=1$. Both parameters τ_c and p are related to the kinetics of the particle aggregation and aggregate breakdown processes. Higher p values imply that particle aggregates are more sensitive to shear, so that their size decreases with increasing shear stress more sensibly. Higher τ_c values indicate that higher shear stresses must be applied in order to attain an appreciable breakdown of particle aggregates.

Eq. 17 is suitable to describe both shear thinning and plastic behavior. In fact, as the shear stress decreases, the size distribution of the aggregate population becomes larger (N_{max} increases), and, correspondingly, also the structural parameter C_{fp} and the effective volume fraction of the disperse phase Φ_{eff} increase. At low enough shear stress, Φ_{eff} may become equal to Φ_m, so that the particle aggregates touch to form a continuous 3D network and the viscosity becomes infinite. The corresponding stress represents the yield stress τ_y. The yield condition is attained only when the volume fraction of the disperse phase Φ is sufficiently high to exceed a limiting value Φ_y. The increase of τ_y with Φ can be derived directly from Eq. (17), but, more conveniently, it can be described with good approximation by the following simple relationship:

$$\tau_y=k_\tau\left(\frac{\Phi-\Phi_y}{\Phi_m-\Phi}\right)^{r} \tag{18}$$

Φ_y marks the transition from shear thinning to plastic behavior within a given class of aggregated suspensions. The less dense are the aggregates, the lower is the Φ_y value.

Figs. 3 and 4 report the profiles of the relative viscosity as a function of the reduced shear stress $\tau_R=\tau/\tau_c$ for two series of DA suspensions and BCCA suspensions, respectively, in a Φ range encompassing the yield condition. As expected,

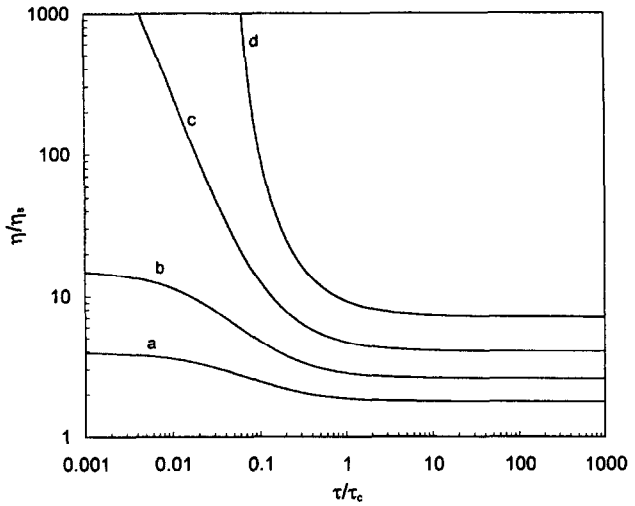

Fig. 3. Relative viscosity curves predicted from Eq. (17) for DA at $\Phi=0.1$ (a), 0.2 (b), 0.3 (c) and 0.4 (d).

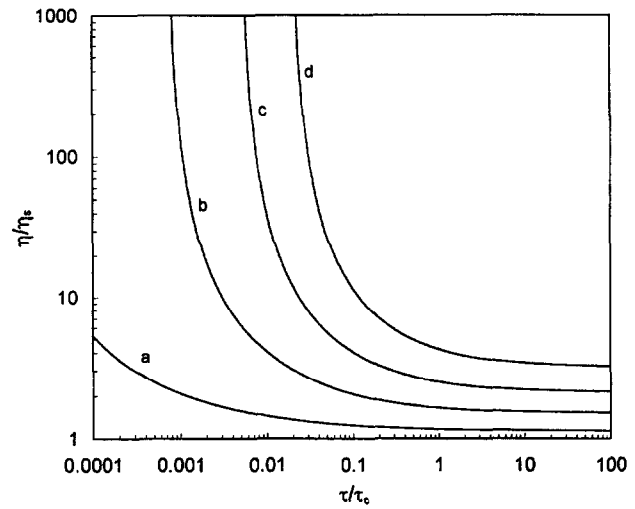

Fig. 4. Relative viscosity curves predicted from Eq. (17) for BCAA at $\Phi=0.05$ (a), 0.15 (b), 0.25 (c) and 0.4 (d).

the model predict the transition from shear thinning to plastic behavior at lower concentration for BCCA suspensions, whose aggregated phase is less dense and representative of several colloidal systems.

3. Experimental validation of the model

In order to check the suitability of the model for describing and interpreting the shear-dependent behavior of aggregated suspensions, the experimental data obtained for two series of epoxy–acrylic systems at different concentrations have been examined. For both series the continuous phase is given by a solution of acrylic resin Luprenal LR 8841 (Basf AG) and epoxy resin DER 331 (Dow Chemical Europe S.A.) in a solvent mixture (butyl glycol, butyl glycol acetate, propyl glycol acetate and Solvesso 150). The disperse phase is composed of titanium dioxide Kronos 2310 (Kronos Titan Gmbh) (series A), and of a mixture of titanium dioxide Kronos 2310 (Kronos Titan Gmbh) and aluminum silicate P820 (Degussa) at a volume ratio 80/20 (series B). Suspensions were prepared at different volume fractions of the disperse phase Φ in the ranges 0.24–0.40 (series A) and 0.16–0.32 (series B), respectively. SEM analyses performed on samples of both series revealed the presence of particle aggregates, which are more extended and less dense for series B. The experimental viscosity data have been determined with a controlled stress rheometer Carri-Med CSL 100 at 20 °C. A detailed description of the experimental procedure is reported elsewhere [37].

All the systems exhibit marked non-Newtonian properties: as the shear stress is increased, the viscosity firstly decreases to reach a minimum condition, and then shear thickening behavior appears above a critical stress. This transition from shear thinning to shear thickening is particularly evident at higher volume fractions and can be ascribed to a reordering process that particles and/or stable aggregates undergo in high shear conditions. In the low-medium τ range the shear-dependent behavior is essentially connected with the aggregation state of the disperse phase and its variations when the shear stress is changed. For this reason, only the experimental data relative to the shear thinning region up to the transition stress have been taken into consideration to check the validity of the proposed model.

Experimental data were correlated by assuming that $\bar{B}$, $\bar{A}$ and $\bar{\beta}$ can vary linearly between the extreme values corresponding to the two limiting cases of dense and fractal aggregates, DA and BCCA, respectively, as follows:

$$\bar{B}=12.4-(12.4-1.574)x \tag{19}$$

$$\bar{A}=1.986-(1.986-0.76)x \tag{20}$$

$$\bar{\beta}=0.538x \tag{21}$$

The parameter x varies between 0(DA) and 1 (BCCA), and is inversely proportional to the density of particle aggregates. Eq. (21) yields a correlation between x and the fractal dimension D:

$$D=\frac{3}{0.538x+1} \tag{22}$$

Accordingly, the adjustable parameters reduce only to x (or D), $N_{max,\infty}$, τ_c and p. The excellent quality of data fitting in the shear stress range which precedes the onset of shear thickening is clearly illustrated by the examples reported in Figs. 5 and 6. This stress range is more extended for system B and practically covers the entire experimental window, while its upper limit is around 10 Pa for system A. System B exhibits plastic behavior, at even the lowest concentration examined ($\Phi=0.16$), whereas an appreciable yield stress is predicted by the model only for the system A at the highest concentration ($\Phi=0.40$).

Figs. 7 and 8 show the variation of D, $N_{max,\infty}$, τ_c and p with increasing Φ for both series. Appreciable between the two series can be noticed for the limiting values $N_{max,\infty}$, the critical stresses τ_c and the D values. We can argue that the disperse

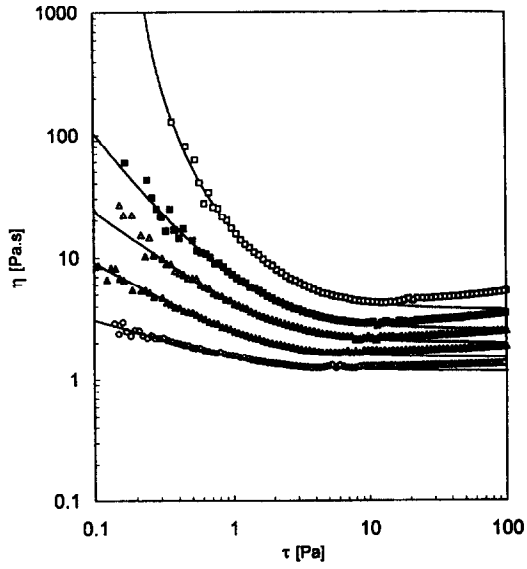

Fig. 5. Comparison between experimental data for system A at different volume fractions (Φ=0.40 (□), 0.36 (■), 0.32 (△), 0.28 (▲), and 0.24 (○)) and flow curves calculated according to Eq. (17).

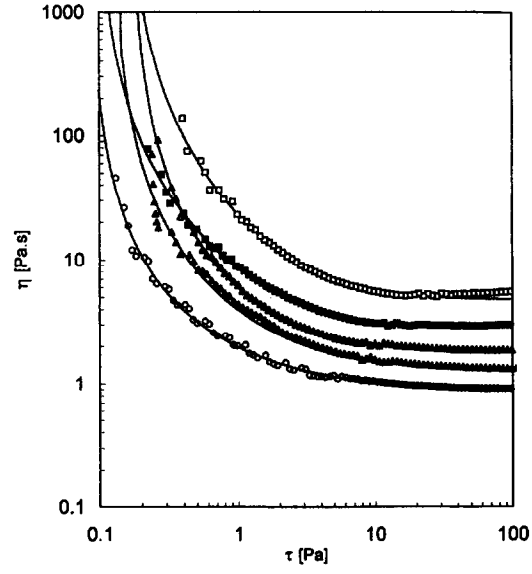

Fig. 6. Comparison between experimental data for system B at different volume fraction (Φ=0.32 (□), 0.28 (■), 0.24 (△), 0.20 (▲), and 0.16 (○)) and flow curves calculated according to Eq. (17).

phase of titanium dioxide suspension A is composed of more compact aggregates (characterized by higher D values), which undergo an appreciable breakdown even at relatively low stresses (τ_c values are lower for system A), so approaching an asymptotic condition characterized by smaller residual aggregates (lower $N_{max,\infty}$ values) for $\tau \rightarrow \infty$. For both systems A and B the aggregate density increases as the concentration of the disperse phase increases. All these conclusions appear to be in accordance with experimental results obtained from SEM analyses.

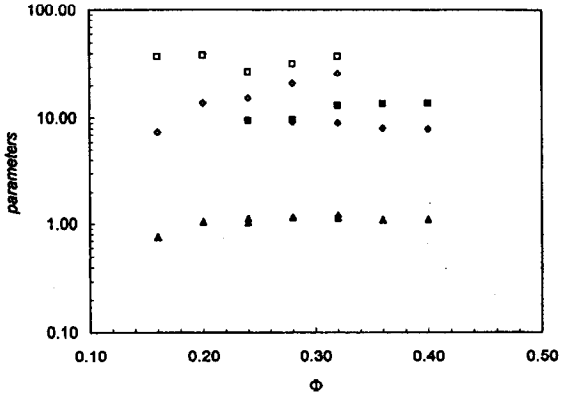

Fig. 7. Model parameters ($N_{max,\infty}$ (diamonds), τ_c (squares), p (triangles)) vs. volume fraction Φ for systems A (filled symbols) and B (open symbols).

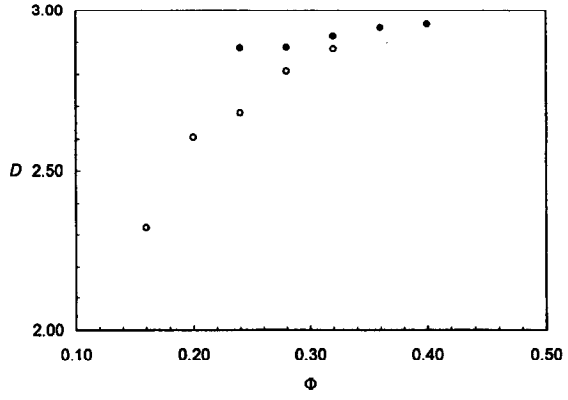

Fig. 8. Fractal dimensionally D vs. volume fraction Φ for systems A (●) and B (○).

4. Conclusions

Rheological modelling of aggregate suspensions implies the definition of an equation able to describe the dependence of the viscosity on the shear stress and on the disperse phase concentration.

The modelling procedure proposed in the present paper can be suitably divided into three steps, the first concerning the choice of an adequate functional dependence of relative viscosity on the disperse phase concentration.

In fact, the viscosity of the suspension is expressed as the product of two contributions: the viscosity of the continuous phase and the relative viscosity, which characterizes the contribution of the disperse phase. At any shear rate, the relative viscosity depends on the effective volume fraction of the disperse phase Φ_{eff}, for aggregated suspensions, or equivalently, on the product $C_{fp}\Phi$, where Φ is the nominal volume fraction.

The second step concerns the characterization of the disperse phase and implies the definition of the dependence of C_{fp}, which is a measure of the degree of aggregation of the disperse phase, on the maximum number of particles per aggregate N_{max}. The correlation derived from the analysis of both real aggregates of sintered glass particles and fractal

aggregates obtained by computer simulation (according to the ballistic cluster–cluster mechanism) leads to a simple common relationships for the variation of C_{fp} with n_i (number of particles per aggregate) which is valid also when aggregate size ranges from that of primary particles to that of fractal objects. In the case of monosized spherical aggregates, the value of C_{fp} for the global suspension coincides with that of each single cluster. Nevertheless, the real situation is characterized by an aggregate size distribution $v_i(n_i)$, an expression is obtained for the dependence of C_{fp} on N_{max}, which contains a parameter β related to the density and, hence, to the fractal dimension of the aggregates.

In the final step the dependence of N_{max} on the shear stress is derived from a rate equation which expresses the balance between the particle aggregation and aggregate breakdown processes.

All the viscosity curves calculated from the model, both for dense and fractal aggregates, closely resemble those observed in real colloidal and non-colloidal suspensions. Thus, the proposed model appears to be suitable to describe and predict the shear viscosity in a wide range of structural conditions of the disperse phase, from fractal aggregates to primary particle. This is confirmed by the analysis of experimental viscosity data relative to two series of epoxy–acrylic systems, containing titanium dioxide and aluminum silicate at different phase concentrations.

Acknowledgements

The authors wish to acknowledge the Italian Ministry for University and Scientific Research for financial support (MURST 60%).

References

[1] A.L. Graham, R.D. Steele and R.B. Bird, *Ind. Eng. Chem. Fundam., 23* (1984) 420.
[2] M.J. Vold, *J. Colloid Sci., 18* (1963) 684.
[3] D.N. Sutherland, *J. Colloid Interface Sci., 25* (1967) 373.
[4] I. Goodarz-Nia and D.N. Sutherland, *Chem Eng. Sci., 30* (1975) 407.
[5] Y.A. Witten and L.M. Sander, *Phys. Rev. Lett., 47* (1981) 1400.
[6] P. Meakin, *J. Colloid Interface Sci., 96* (1983) 415.
[7] M. Kolb and R. Jullien, *J. Phys. Lett., 45* (1984) L977.
[8] R. Jullien and M. Kolb, *J. Phys., A17* (1984) L639.
[9] D.A. Wetz and M. Oliveria, *Phys. Rev. Lett., 52* (1984) 1433.
[10] D.S. Wetz, M.Y. Lin, J.S. Huang, T.A. Witten, S.K. Sinha and J.S. Gethner, in R. Pynn and A. Skjeltorp (eds.), *Scalling Phenomena in Disordered Systems*, Plenum Press, New York, 1985, p. 171.
[11] W.D. Brown and R.C. Ball, *J. Phys., A18* (1985) L517.
[12] M. Kolb, *Physica, 140A* (1986) 416.
[13] R. Jullien and R. Botet, *Aggregation and Fractal Aggregates*, World Scientific, Singapore, 1987.
[14] P. Meakin and F. Family, *Phys. Rev., A36* (1987) 5498.
[15] H.M. Lindsay, M.Y. Lin, D.A. Weitz, P. Sheng, Z. Chen, R. Klein and P. Meakin, *Faraday Discuss. Chem. Soc., 83* (1987) 153.
[16] P. Meakin, *Ann. Rev. Phys. Chem., 39* (1988) 237.
[17] P. Meakin, *Adv. Colloid Interface Sci., 28* (1988) 249.
[18] M.Y. Lin, T. Klein, H.M. Lindsay, D.A. Wetz, R.C. Ball and P. Meakin, *J. Colloid Interface Sci., 137* (1990) 263.
[19] M.Y. Lin, R. Klein., H.M. Lindsay, D.A. Wetz, R.C. Ball and P. Meakin, *Phys. Rev., A41* (1990) 2005.
[20] T. Vicsek, *Fractal Growth Phenomena*, World Scientific, Singapore, 1993.
[21] D. Quemada, *Rheol. Acta, 16* (1977) 82; *Rheol. Acta, 17* (1978) 632.
[22] I.M. Krieger and T.J. Dougherty, *Trans. Soc. Rheol., 3* (1959) 137.
[23] H.A. Barnes, *Theoretical and Applied Rheology, Proc. XIth Int. Congr. on Rheology, Brussels, August 1992*, Elsevier, Amsterdam, 1992, p. 576.
[24] A. Potanin and N.B. Uriev, *J. Colloid Interface Sci., 142* (1990) 385.
[25] R. Lapasin, *Chem. Biochem. Eng. Q., 1* (1987) 143.
[26] R. Lapasin, M. Grassi and S. Pricl, in G. Biardi, M. Giona and A.R. Giona (eds.) *Chaos and Fractal in Chemical Engineering*, World Scientific, Singapore, 1995, p. 89.
[27] D.F. Bagster and D. Tomi, *Chem. Eng. Sci., 29* (1974) 1773.
[28] D. Tomi and D.F. Bagster, *Chem. Eng. Sci., 30* (1975) 269.
[29] P.M. Adler, *Rheol. Acta., 17* (1978) 288.
[30] P.M. Adler and P.M. Mills, *J. Rheol., 23* (1979) 25.
[31] R.J. Hunter and J. Frayne, *J. Colloid Interface Sci., 76* (1980) 107.
[32] R.C. Sonntag and W.B. Russel, *J. Colloid Interface Sci., 113* (1986) 399.
[33] R.C. and Sonntag and W.B. Russel, *J. Colloid Interface Sci., 115* (1987) 378.
[34] L.B. Brakalov, *Chem. Eng. Sci., 42* (1987) 2373.
[35] A.A. Potanin, *J. Chem. Phys., 96* (1992) 9191.
[36] A.A. Potanin, *J. Colloid Interface Sci., 157* (1993) 399.
[37] A. Zupancic, *Ph.D. Thesis*, Ljubljana, 1995.